Theoretical Study on the Mechanism for the Addition Reaction of SiH_3 with Propylene and Acetic Acid

Yongjun Liu,*,†,‡,§ Zhiguo Wang,‡ and Yourui Suo§

School of Chemistry and Chemical Engineering, Shandong University, Jinan, Shandong, 250100, China, Department of Chemistry, Qufu Normal University, Qufu, Shandong, 273165, China, and Northwest Institute of Plateau Biology, Chinese Academy of Sciences, Xining, Qinghai, 810001, China

Received: June 10, 2006; In Final Form: August 22, 2006

To explore the reactivities of alkene (−CH═CH_2) and carboxy (−COOH) group with H−Si under UV irradiation, the addition mechanism for the reactions of SiH_3 radical with propylene and acetic acid was studied by using the B3LYP/6-311++G(d,p) method. Based on the surface energy profiles, the dominant reaction pathways can be established; i.e., SiH_3 adds to the terminal carbon atom of the alkene (−CH═CH_2) to form an anti-Markovnikov addition product, or adds to the oxygen atom of the carboxy group (−COOH) to form silyl acetate (CH_3−COOSiH_3). Because the barrier in the reaction of the carboxy group (39.9 kJ/mol) is much larger than that of alkene (11.97 kJ/mol), we conclude that the reaction of bifunctional molecules (e.g., ω-alkenoic acid) with H−Si under irradiation condition is highly selective; i.e., the alkene group (−CH═CH_2) reacts with SiH_3 substantially faster than the carboxyl group (−COOH), which agrees well with the experimental results. This provides the possibility of preparing carboxy-terminated monolayers on silicon surface from ω-alkenoic acids via direct photochemical reaction.

Introduction

Ordered organic monolayer films on silicon surfaces have received much attention not only for industrial purposes but also because of scientific interest.[1−8] Since the seminal work reported by Chidsey and co-workers a decade ago, many methods for preparing hybrid organic−silicon systems have been developed, involving wet chemical and ultrahigh-vacuum (UHV) approaches.[9−26] Among these, a particularly promising approach is a radical-initiated reaction of terminally unsaturated molecules with a hydrogen-terminated silicon surface because of its simplicity in operation, mild reaction conditions, and high selectivity. It has been inferred that this surface reaction occurs via a chain mechanism;[12,13] i.e., after abstracting a hydrogen atom from a neighboring Si−H unit, alkene/alkyne molecules react with the silicon dangling bond to form an intermediate carbon radical state, which abstracts a hydrogen atom from a neighboring Si−H unit to form a stable adsorbed species plus a new Si dangling bond.

Very recently, Yu[27] and Boukherroub[28,29] explored the reaction of bifunctional molecules (e.g., ω-alkenoic acid) with hydrogen-terminated silicon (Figure 1). They demonstrated experimentally that the alkene group (−CH═CH_2) reacts with hydrogen-terminated silicon substantially faster than the carboxyl group (−COOH). This affords a facile method to prepare ω-carboxylic group terminated silicon surfaces, which has enormous potential for biotechnological applications such as the fabrication of silicon-based DNA chips.

On the theoretical side, some density functional theoretical calculations have been carried out for the reactions of alkene with H−Si(100)[4,30−35] and H−Si(111),[13,36,37] using slab or cluster models. However, a comparable study of alkene (−CH═CH_2) and carboxy group (−COOH) is still required.

* Corresponding author. Telephone: 0531-88365576. Fax: 0531-88564464. E-mail address: yongjunliu_1@sdu.edu.cn.
† Shandong University.
‡ Qufu Normal University.
§ Chinese Academy of Sciences.

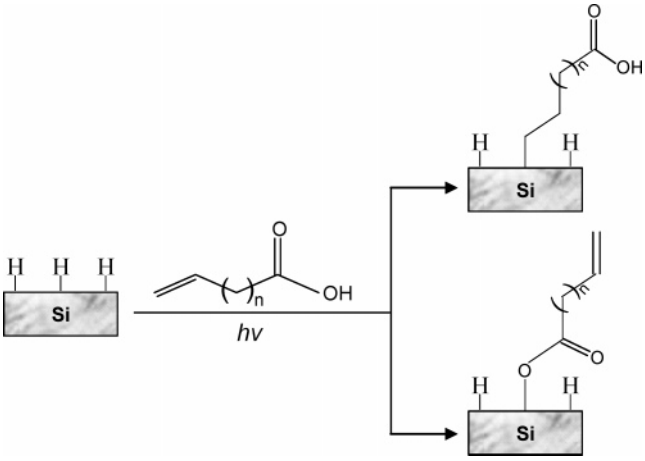

Figure 1. Schematic illustration of the two possible orientations when ω-alkenoic acids react with hydrogen-terminated silicon (H−Si).

The present paper gives a first-principles investigation of the reaction of alkene (propylene) and carboxy group (acetic acid) with SiH_3 radical, which provides fundamentals involving optimized structures, the reaction pathway, and relative energies.

Computational Method

All calculations were carried out by using the Gaussian 98 program package. The geometric parameters of the reactants, intermediates, and transition states were fully optimized at the B3LYP/6-311++G(d,p) level and confirmed by vibrational analysis. On a potential energy surface all optimized geometries correspond to a local minimum that has no imaginary frequency mode or to a saddle point that has only one imaginary frequency mode.

Result and Discussion

In this study, we have considered two kinds of reaction pathways for the reactions of both propylene and acetic acid

10.1021/jp063623t CCC: $33.50
Published on Web 10/20/2006

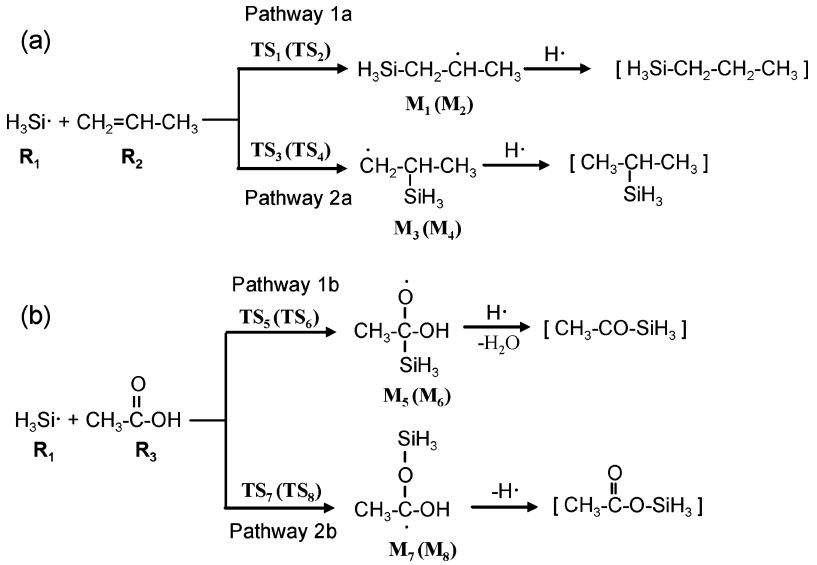

Figure 2. Possible reaction pathways for reactions of SiH_3 radical with $-CH{=}CH_2$ and $-COOH$ functional groups. (a) SiH_3 with propylene; (b) SiH_3 with acetic acid.

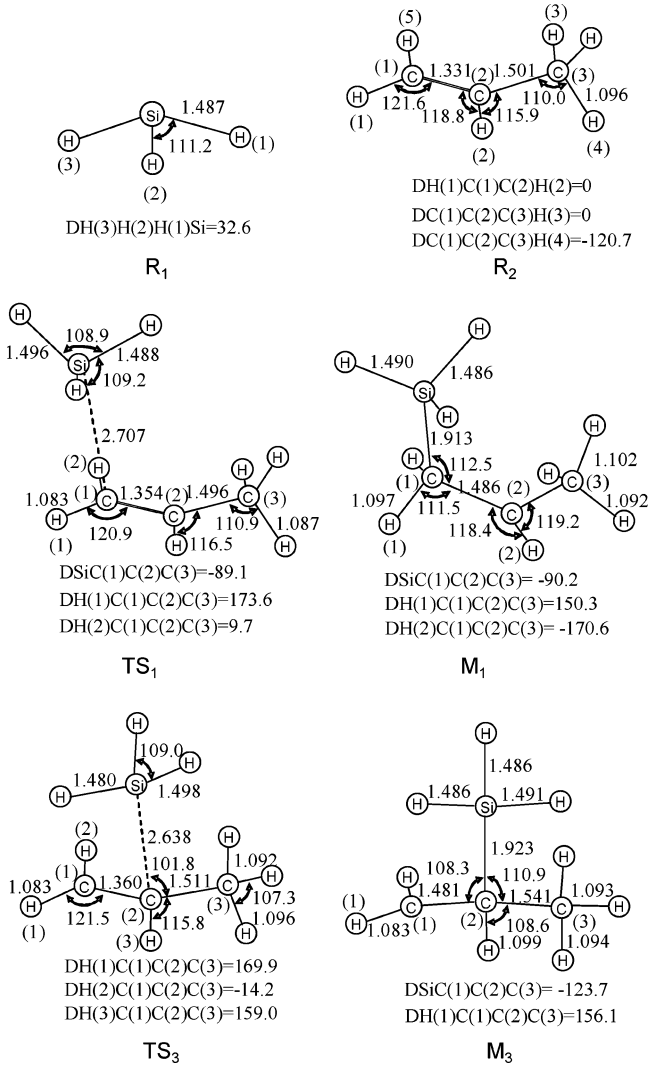

Figure 3. Optimized geometric parameters for species in the addition reaction of SiH_3 with propylene at B3LYP/6-311++G(d,p) level. Lengths are in 0.1 nm and angles are in degrees.

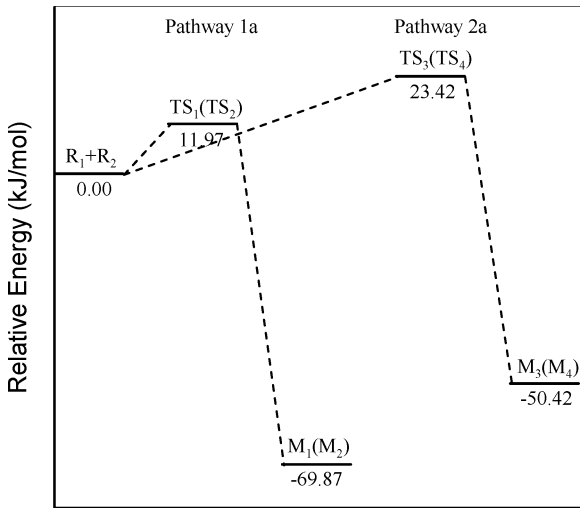

Figure 4. Profile of potential energy surface for the addition reaction of propylene with SiH_3 at B3LYP/6-311++G(d,p) level.

with SiH_3 radical, as shown in Figure 2. For the reaction of propylene, SiH_3 reacts either with the terminal carbon atom to form secondary carbon radicals M_1 and M_2 via transition states TS_1 and TS_2 or with a middle carbon atom to form terminal carbon radicals M_3 and M_4 via transition states TS_3 and TS_4, respectively. In the reaction of acetic acid, SiH_3 reacts with either the carbon or oxygen atom of the carboxy group as shown in pathways 1b and 2b, respectively. The pathway of silyl radical attacking the hydroxyl oxygen in the carboxylic acid was also examined. However, our calculation results indicated that this pathway does not lead to any transition state or intermediate.[38]

Propylene. The optimized structures of the reactants R_1 (SiH_3) and R_2 (propylene), transition states (TS_1 and TS_3), and intermediates (M_1 and M_3) are shown in Figure 3. For the structure of propylene (R_2), we used the most stable conformation shown in Figure 3. The profile of the potential energy surface is shown in Figure 4.

As shown in Figures 3 and 4, two reaction pathways, 1a and 2a, were considered in the reaction of propylene. When SiH_3 radical attacks the terminal carbon atom (C_1) of the alkene group ($-CH{=}CH_2$) from the upper side of the plane H(1)H(2)C(1), the transition state TS_1 will be formed. In transition state TS_1, the optimized $Si-C_1$ distance is 2.707 Å and the C_1-C_2 bond length changed from 1.331 to 1.354 Å. Because of the

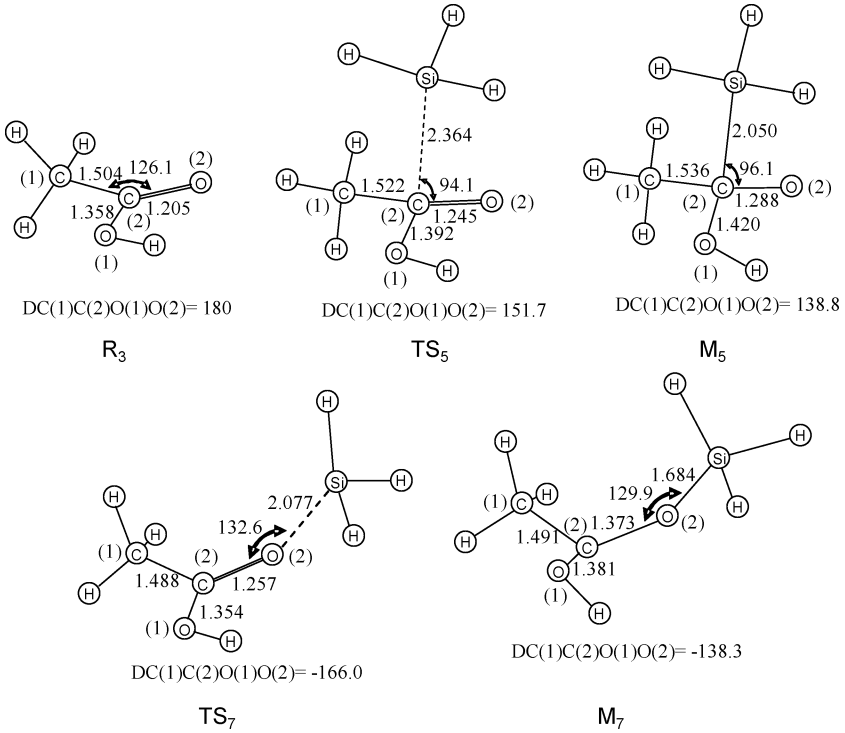

Figure 5. Optimized geometric parameters for species in the addition reaction of SiH_3 radical with acetic acid at B3LYP/6-311++G(d,p) level. Lengths are in 0.1 nm and angles are in degrees.

interaction between SiH_3 and C_1 atom, the dihedral of H(1)C(1)C(2)C(3) and H(2)C(1)C(2)C(3) changed from 180° and 0° to 173.6° and 9.7°, respectively. The unique imaginary frequency of the transition state TS_1 is 216.0i cm^{-1}, which therefore affirms the transition state TS_1 as a real one. Calculations of intrinsic reaction coordinates (IRC) and further optimization of the primary IRC results indicated that TS_1 connects the reactants (R_1 and R_2) and an intermediate (secondary carbon radical) (M_1).[39]

In intermediate M_1, the distance between Si and C_1 decreased to 1.913 from 2.707 Å, and the dihedral of H(1)C(1)C(2)C(3) changed from 173.6° to 150.3°. Because of the high reactivity, M_1 reacts readily with H radical to form the anti-Markovnikov product with a barrier-free reaction. (The results are not shown.) If the SiH_3 radical attacks the terminal carbon atom (C_1) from the other side of the plane H(1)H(2)C(1), another transition state (TS_2) and intermediate (M_2) will be formed (the structures are not shown), which are isomers of TS_1 and M_1, respectively.

Figures 3 and 4 also show that SiH_3 may react with the middle carbon atom (C_2) to form transition states (TS_3 and TS_4) and intermediates (M_3 and M_4). TS_4 and M_4 are the isomers of TS_3 and M_3, respectively. The unique imaginary frequency of transition state TS_3 or TS_4 is 290.6i cm^{-1}, which affirms the two transition states as the real ones. According to the calculation of IRC and further optimization of the primary IRC results, TS_3 and TS_4 connect reactants R_1 and R_2 and intermediates M_3 and M_4, respectively.

A comparison between the two reaction pathways indicates that two reaction pathways compete with each other. The barrier of TS_3/TS_4 in pathway 2a is 11.45 kJ/mol higher than that of TS_1/TS_2 in pathway 1a. According to the exponential law of reaction velocity, the reaction velocity from TS_1/TS_2 to M_1/M_2 is approximately 102 times as fast as that from TS_3/TS_4 to M_3/M_4 at normal temperature. Therefore, the dominant reaction

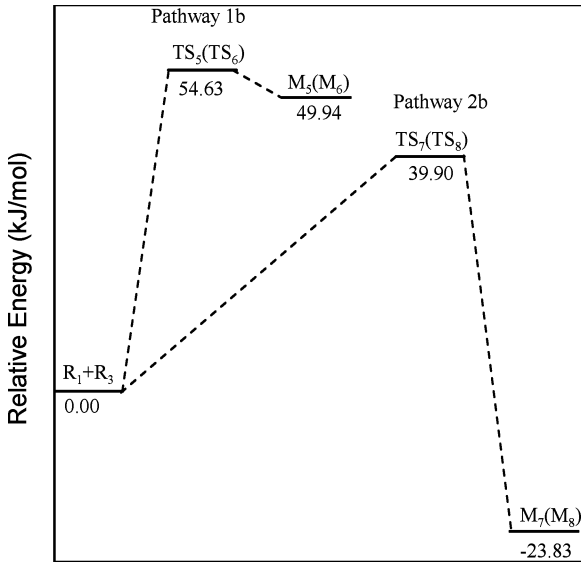

Figure 6. Profile of potential energy surface for the addition reaction of acetic acid with SiH_3 at B3LYP/6-311++G(d,p) level.

pathway is the addition of SiH_3 with the terminal carbon of the alkene group (−CH═CH_2) and the anti-Markovnikov products could be obtained, which is consistent with the experimental results.[40]

Acetic Acid. To compare the reactions of SiH_3 with propylene and acetic acid, two possible reaction pathways (1b and 2b) in the reaction of acetic acid were examined. The optimized structures of the reactant R_3 (acetic acid), transition states (TS_5 and TS_7), and intermediates (M_5 and M_7) are shown in Figure 5. For the structures of acetic acid, we used the most stable conformation. The profile of potential energy surface is shown in Figure 6.

As shown in Figures 5 and 6, when SiH_3 attacks the carbon atom (C_2) of the carboxy group (−COOH), transition states TS_5/

TS_6 will be formed with the barrier of 54.63 kJ/mol. Because of its larger barrier, the dominant reaction pathway should be 2b.

In pathway 2b, transition states TS_7/TS_8 were first formed when SiH_3 attacks the oxygen atom of the carboxy group. In transition state TS_7, the optimized $Si-O_2$ distance is 2.077 Å, which is a little longer than the $Si-C_2$ distance in transition state TS_5. We can also see the change of the C_2-O_2 bond length. In TS_7, the C_2-O_2 bond length changed from 1.205 (in R_3) to 1.257 Å (in TS_7); i.e., with increasing interaction between SiH_3 and the O_2 atom, the C_2-O_2 bond has the tendency to become a single bond. The dihedral of C(1)C(2)O(1)O(2) changed from 180° to −166.0°, implying the transfer of the hybridization of C_2 from SP^2 to SP^3. The unique imaginary frequency of the transition state TS_7/TS_8 is 433.7i cm^{-1}; which affirms the transition states TS_7/TS_8 as the real ones. The IRC calculation results of TS_7/TS_8 indicate that TS_7/TS_8 connect the reactants (R_1 and R_3) and intermediates (M_7/M_8).[39]

According to the exponential law of reaction velocity, the reaction velocity from TS_7/TS_8 to M_7/M_8 is approximately 334 times as fast as that from TS_5/TS_6 to M_5/M_6 at normal temperature. Therefore, the dominant reaction pathway is the addition of SiH_3 with the oxygen in the carboxy group. The small barrier from TS_7/TS_8 to M_7/M_8 indicates that in the gas phase silyl radical reacts readily with carboxylic acid leading to the silyl ester ($CH_3-COOSiH_3$). In addition, it is well-known that hydrogen-terminated silicon surface can be activated by cleaving the Si−H bond under UV irradiation. Each dangling bond on the surface is very similar to a Si-substituted silyl radical. Ignoring the substituent effect, we predicted that hydrogen-terminated silicon surface can react with carboxylic acids leading to esters. In fact, the reaction of undecylenic acid with hydrogen-terminated silicon in solution has been proved experimentally.[27]

From the above calculation results, we conclude that both alkene and carboxy groups react with SiH_3 radical. The different barrier energies for alkene and carboxy groups when reacting with silyl radical suggested, from a thermodynamic point of view, that the reaction between alkene and SiH_3 is faster than that of carboxylic acid and SiH_3. It has been observed experimentally by the photochemical reactions of H−Si(111) with *n*-alkenes and alkanoic acids.[27] The reaction with *n*-alkenes yields closely packed monolayers, while alkanoic acids react with H−Si(111) slowly and incompletely. By using the reaction of *ω*-alkenoic acids with hydrogen-terminated silicon surface, carboxy-terminated monolayers on silicon surface could be obtained.[27]

Conclusion

The radical mechanism for the addition reactions of propylene and acetic acid with SiH_3 were studied by using the B3LYP/6-311++G(d,p) method. Based on the surface energy profiles, the dominant reaction pathways can be established; i.e., SiH_3 reacts with the terminal carbon atom of alkene ($-CH=CH_2$) to form the anti-Markovnikov addition product, or with the oxygen in the carboxy group (−COOH) to form silyl acetate ($CH_3-COOSiH_3$). By comparing the barriers in the reaction of carboxy group (39.9 kJ/mol) and in the reaction of alkene (11.97 kJ/mol), we conclude that the reaction between SiH_3 and a bifunctional (e.g., *ω*-alkenoic acid) molecule is highly selective.

Acknowledgment. This work was supported by New Faculty Start-up Funds of Shandong University and the Program of Hundreds Talent of the Chinese Academy of Sciences.

Supporting Information Available: Detailed description of the potential energy surface profile and the results of IRC calculation. This material is available free of charge via the Internet at http://pubs.acs.org.

References and Notes

(1) Rakshit, T.; Liang, G.-C.; Ghosh, A. W.; Datta, S. *Nano Lett.* **2004**, *4*, 1803.
(2) Sieval, A. B.; Linke, R.; Zuihof, H.; Sudhölter, E. J. R. *Adv. Mater.* **2000**, *12*, 1457.
(3) Wayner, D. D. M.; Wolkow, R. A. *J. Chem. Soc., Perkin Trans. 2* **2002**, 23.
(4) Lopinsky, G. P.; Wayner, D. D. M.; Wolkow, R. A. *Nature (London)* **2000**, *406*, 48.
(5) Buriak, J. M. *Chem. Rev.* **2002**, *102*, 1271.
(6) Hamers, R. J.; Coulter, S. K.; Ellison, M. D.; Jovis, J. S.; Padowitz, D. F.; Schwartz, M. P.; Greenlief, C. M.; Russel, J. N., Jr. *Acc. Chem. Res.* **2000**, *33*, 617.
(7) Wolkow, R. A. *Annu. Rev. Phys. Chem.* **1999**, *50*, 413.
(8) Jin, J.; Wang, G.; Yang, W.-S.; Liu, G.-Z.; Li, T. J. *Chin. J. Chem.* **2003**, *21*, 1517.
(9) Linford, M. R.; Chidsey, C. E. D. *J. Am. Chem. Soc.* **1993**, *115*, 12631.
(10) Linford, M. R.; Fenter, P.; Eisenberger, P. M.; Chidsey, C. E. D. *J. Am. Chem. Soc.* **1995**, *117*, 3145.
(11) Wagner, P.; Nock, S.; Spudich, J. A.; Volkmuth, W. D.; Chu, S.; Cicero, R. L.; Wade, C. P.; Linford, M. R.; Chidsey, C. E. D. *J. Struct. Biol.* **1997**, *119*, 189.
(12) Cicero, R. L.; Lindord, M. R.; Chidsey, C. E. D. *Langmuir* **2000**, *16*, 5688.
(13) Cicero, R. L.; Chidsey, C. E. D.; Lopinsky, G. P.; Wayer, D. D. M.; Wolkow, R. A. *Langmuir* **2002**, *18*, 305.
(14) Sieval, A. B.; Demirel, A. L.; Nissink, J. W. M.; Linford, M. R.; van der Maas, J. H.; de Jeu, W. H.; Zuilhof, H.; Sudhölter, E. J. R. *Langmuir* **1998**, *14*, 1759.
(15) Sieval, A. B.; Vleeming, V.; Zuilhof, H.; Sudhölter, E. J. R. *Langmuir* **1999,** *15*, 8288.
(16) Sieval, A. B.; Linke, R.; Heij, G.; Meijer, G.; Zuilhof, H.; Sudhölter, E. J. R. *Langmuir* **2001**, *17*, 7554.
(17) Boukherroub, R.; Morin, S.; Bensebaa, F.; Wayner, D. D. M. *Langmuir* **1999**, *15*, 3831.
(18) Boukherroub, R.; Wayner, D. D. M. *J. Am. Chem. Soc.* **1999**, *121*, 11513.
(19) Henry de Villeneuve, C.; Pinson, J.; Bernard, M. C.; Allongue, P. *J. Phys. Chem. B* **1997**, *101*, 2415.
(20) Allongue, P.; Henry de Villeneuve, C.; Pinson, J.; Ozanam, F.; Chazalviel, J. N.; Wallart, X. *Electrochim. Acta* **1998**, *43*, 2791.
(21) Fidelis, A.; Ozanam, F.; Chazalviel, J.-N. *Surf. Sci.* **2000**, *444*, L7.
(22) Teyssot, A.; Fidelis, A.; Fellah, S.; Ozanam, F.; Chazalviel, J.-N. *Electrochim. Acta* **2002**, *47*, 2565.
(23) Bansal, A.; Li, X.; Lauermann, I.; Lewis, N. S.; Yi, S. I.; Weinberg, W. H. *J. Am. Chem. Soc.* **1996**, *118*, 7225.
(24) Bansal, A.; Lewis, N. S. *J. Phys. Chem. B* **1998**, *102*, 1067.
(25) Haber, J. A.; Lauermann, I.; Michalak, D.; Vaid, T. P.; Lewis, N. S. *J. Phys. Chem. B* **2000**, *104*, 9947.
(26) Liu, Y.-J.; Navasero, N. M.; Yu, H.-Z. *Langmuir* **2004**, *20*, 4039.
(27) Asanuma, H.; Lopinski, G. P.; Yu, H.-Z. *Langmuir* **2005**, *21*, 5013.
(28) Boukherroub, R.; Wojtyk, J. T. C.; Wayner, D. D. M.; Lockwood, D. J. *J. Electrochem. Soc.* **2002**, *149*, H59−H63.
(29) Boukherroub, R.; Petit, A.; Loupy, A.; Chazalviel, J.-N.; Ozanam, F. *J. Phys. Chem. B* **2003**, *107*, 13459−13462.
(30) Sieval, A. B.; Optiz, R.; Maas, H. P. A.; Shoeman, M. G.; Meijer, G.; Vergeldt, F. J.; Zuilhof, H.; Sudholter, E. J. R. *Langmuir* **2000**, *16*, 10359.
(31) Kang, J. K.; Musgrave, C. B. *J. Chem. Phys.* **2002**, *116*, 9907.
(32) Kruse, P.; Johnson, E. R.; Dilabio, G. A.; Wolkow, R. A. *Nano Lett.* **2002**, *2*, 807.
(33) Tong, X.; DiLabio, G. A.; Clarkin, O. J.; Wolkow, R. A. *Nano Lett.* **2004**, *4*, 357.
(34) Tong, X.; DiLabio, G. A.; Wolkow, R. A. *Nano Lett.* **2004**, *4*, 979.
(35) Cho, J.-H.; Oh, D.-H.; Kleinman, L. *Phys. Rev. B* **2002**, *65*, 081310-(R).
(36) Pei, Y.; Ma, J.; Jiang, Y.-S. *Langmuir* **2003**, *19*, 7652.
(37) Lu, X.; Wang, X.-L.; Yuan, Q.-H.; Zhang, Q.-E. *J. Am. Chem. Soc.* **2003**, *125*, 7923.
(38) For a detailed description of the potential energy surface profile, see the Supporting Information.
(39) For the results of IRC calculation, see the Supporting Information.
(40) Kopping, B.; Chatgilialoglu, C.; Zehnder, M.; Giese, B. *J. Org. Chem.* **1992**, *57*, 3994.